HHS Public Access

Author manuscript

Nat Struct Mol Biol. Author manuscript; available in PMC 2009 November 12.

Published in final edited form as:

Nat Struct Mol Biol. 2009 March ; 16(3): 255–264. doi:10.1038/nsmb.1556.

A Complex Gene Regulatory Mechanism that Operates at the Nexus of Multiple RNA Processing Decisions

David S. McPheeters[1], **Nicole Cremona**[1], **Sham Sunder**[1], **Huei-Mei Chen**[2], **Nicole Averbeck**[2], **Janet Leatherwood**[2], and **Jo Ann Wise**[1]

[1]Center for RNA Molecular Biology and Department of Molecular Biology & Microbiology, Case Western Reserve University, School of Medicine, Cleveland, Ohio 44106-4960

[2]Department of Molecular Genetics and Microbiology, State University of New York, Stony Brook, NY 11794-5222

Abstract

Expression of *crs1* pre-mRNA, encoding a meiotic cyclin, is blocked in actively growing fission yeast cells by a multifaceted mechanism. The most striking feature is that *crs1* transcripts are continuously synthesized in vegetative cells, but are targeted for degradation rather than splicing and polyadenylation. Turnover of *crs1* RNA requires the exosome, similar to previously described nuclear surveillance and silencing mechanisms, but does not involve a non-canonical poly(A) polymerase. Instead, *crs1* transcripts are targeted for destruction by a factor previously implicated in turnover of meiotic RNAs in growing cells. Like exosome mutants, *mmi1* mutants splice and polyadenylate vegetative *crs1* transcripts. Two regulatory elements are located at the 3′ end of the *crs1* gene, consistent with the increased accumulation of spliced RNA in polyadenylation factor mutants. This highly integrated regulatory strategy may ensure a rapid response to adverse conditions, thereby guaranteeing survival.

INTRODUCTION

Meiosis is a highly conserved cellular differentiation pathway in which one round of DNA synthesis is followed by two successive rounds of division, leading to the formation of haploid cells from diploid precursors1. Although the meiotic cell cycle is similar among eukaryotes, the underlying regulatory mechanisms vary widely. In multicellular organisms, extrinsic cues from surrounding cells stimulate germ cells to enter the differentiation

Correspondence should be addressed to J.A.W. (jaw17@case.edu) Phone: (216)-368-1876, FAX (216)-368-3055.

AUTHOR CONTRIBUTIONS

David McPheeters performed the TRO experiments, designed the real-time PCR assay, and participated in development of the model as well as writing of the manuscript. Nicole Cremona constructed and analyzed the chimeric and mutant alleles of *crs1* to define the regulatory element, performed the RNA analyses on *trans*-acting factor mutants, qPCR, and expertly proofread the manuscript. Sham Sunder analyzed processing of *crs1* RNA over a meiotic time course and conducted initial experiments to map the *crs1* regulatory element. Nicole Averbeck mapped the *crs1* RNA termini by RACE and constructed the *crs1* deletion strain. Huei-Mei Chen and Janet Leatherwood discovered the splicing defect in the *pfs2-11* mutant. Jo Ann Wise wrote the manuscript and contributed to the design and interpretation of all experiments.

Note: Supplementary Information accompanies this article.

pathway, whereas in unicellular organisms such as the budding yeast *Saccharomyces cerevisiae* and the fission yeast *Schizosaccharomyces pombe*, entry into meiosis is triggered by nutrient deprivation. In either case, the decision to initiate sexual differentiation is tightly regulated to prevent execution of this specialized cell cycle under inappropriate conditions or in improper developmental contexts.

At the molecular level, meiosis involves a complex cascade of sequential changes in gene expression1, which in *S. pombe* are due in part to an extensive program of meiosis-specific pre-mRNA splicing2. In contrast to budding yeast, where the transcripts spliced exclusively during meiosis encode proteins involved in chromosome transactions3,4, meiosis-specific splicing controls production of a wide variety of gene products in fission yeast2,5. Moreover, at least for *crs1* and *rem1* RNAs, which encode meiotic cyclins, the block to splicing is biologically relevant, as over-expression in mitotic *S. pombe* cells is toxic2,6.

Although regulated splicing in the form of intron retention precludes production of full-length meiotic proteins in actively growing cells of both yeasts, the underlying control mechanisms appear to be distinct. In *S. cerevisiae*, meiotically spliced RNAs contain intronic enhancer elements that promote splicing via binding to a KH domain RNA binding protein expressed only during meiosis4. In contrast, the three meiotically spliced *S. pombe* transcripts examined to date (*mes1*, *crs1*, and *rem1*) are regulated by non-intronic sequences outside the coding regions, which in both *rem1* and *mes1* reside upstream2,6-8. These observations were reminiscent of the changes in alternative splicing patterns upon switching promoters in metazoans2,8-10. However, the *crs1* regulatory mechanism appeared to be distinct, as the flanking regions were unable to prevent splicing of heterologous introns in mitotically growing fission yeast cells, whereas the *rem1* flanking regions sufficed to impose meiosis-specific splicing on an otherwise constitutively spliced transcript2.

Here, we describe a series of experiments in *S. pombe* designed to illuminate the intricate molecular mechanism underlying *crs1* regulation. As the regulatory sequences lie at the 3′ end of the gene, the mechanism clearly does not involve promoter-driven splicing. The most surprising finding was that increased RNA accumulation during sexual differentiation is not due to up-regulation of *crs1* transcription, but rather mirrors alterations in nuclear RNA processing and turnover. Another unexpected feature of the *crs1* control mechanism is coupling of polyadenylation and splicing, which was previously believed to occur only in mammals11. We propose that the highly integrated *crs1* regulatory strategy serves to “prime” the gene expression pump, allowing a rapid response to adverse conditions that ensures survival.

RESULTS

Accumulation of *crs1* RNA does not reflect transcription

To follow up on our finding that critical splicing regulatory element(s) lie outside the *crs1* coding region2, we set out to determine if transcription of the gene changes during meiosis. To this end, we directly measured RNA synthesis using transcriptional run-on (TRO) assays12 in the temperature-sensitive *pat1–114* mutant, which undergoes ectopic meiosis at the restrictive temperature even as a haploid13. Remarkably, *crs1* transcription was highest

in vegetative cells (0 time point), followed by a steady decline to background levels 5 hr after meiotic induction (Fig. 1a, top). We conclude that the increased accumulation during meiosis must in fact reflect decreased turnover of the RNA. This inference is at odds with the central conclusion from genome-wide microarray and deep-sequencing analyses, which attributed changes in RNA levels between mitotic and meiotic fission yeast cells to transcriptional regulation14-16.

As controls, we performed TRO on two intronless genes. The *pta1* gene, encoding the fission yeast orthologue of the polyadenylation factor symplekin17, displayed a transcription profile similar to *crs1* (Fig. 1a, middle). However, in contrast to the spike in the *crs1* microarray signal, *pta1* RNA accumulation remained constant throughout meiosis14, a pattern typical of constitutive transcripts (including those encoding other core 3′ processing factors). The transcription profile of *meu4*, a meiotic gene of unknown function18, was distinct from both *crs1* and *pta1*, with undetectable synthesis in mitotic cells and a dramatic peak during mid-meiosis (Fig. 1a, bottom).

To determine whether the discrepancy between synthesis and accumulation of *crs1* RNA reflected the altered pattern of splicing observed previously2, we used quantitative real-time PCR (qPCR) with primers designed to distinguish spliced transcripts from those that retained introns (see Supplementary Methods, online). Notably, the 74-fold difference in total steady-state *crs1* RNA levels between vegetative cells and the peak observed during meiosis (∼3 hr post-induction) was attributable almost entirely to an increase in spliced *crs1* RNA (Fig. 1b), consistent with processing, not transcription, determining increased expression during meiosis.

Polyadenylation is activated concurrently with splicing

In light of the unexpected discrepancy between the kinetics of transcription and splicing, we examined 3′ processing of *crs1* RNA over a meiotic time course (Fig. 2a). Remarkably, vegetative transcripts (0 time point) were not only unspliced, but also lacked poly(A) tails. In meiotic cells, two polyadenylated *crs1* species were detected; the larger RT-PCR product peaked at 3 hr, while the smaller one was approximately equal in intensity at 2-4 hr (Fig. 2a). Sequence analysis revealed that the distal *crs1* 3′ end, which predominates, is located within an element that closely resembles mammalian cleavage and polyadenylation signals19,20, while the proximal, minor 3′ end is specified by an element that contains a critical deviation (AAUcAA) from the consensus (AAUAAA) mammalian hexamer21 (Fig. 2b). Intriguingly, the two polyadenylation signals are contiguous (Fig. 2b & c), and use of the wild-type proximal signal was increased by mutating the signature hexanucleotide to consensus (Supplementary Fig. 1 online). In contrast, 5′ RACE indicated that the transcription start site does not change between mitotic and meiotic cells (Fig. 2c).

To confirm that the kinetics of *crs1* polyadenylation and splicing precisely coincide during meiosis, we assayed the same RNA preparations for intron removal (Fig. 2d). Like polyadenylation, splicing peaked at ∼3 hr post-meiotic induction, suggesting that the two RNA processing reactions might be coupled. This inference was confirmed by RT-PCR analysis with a 5′ primer complementary to the first exon and oligo(dT) as the 3′ primer, which demonstrated that individual *crs1* transcripts had either undergone both RNA

processing reactions or were neither spliced nor polyadenylated (Fig. 2e). In further support of coupling between 3′ processing and splicing, unspliced read-through transcripts, but not spliced read-through transcripts, were detected at early time points following meiotic induction (Supplementary Fig. 2 online).

The nearly undetectable level of partially spliced *crs1* RNAs throughout meiosis (Fig. 2d) suggested that splicing of all four *crs1* introns might be coordinately regulated. Consistent with a control mechanism extending throughout the gene, the predominant species detected when splicing was assayed at more frequent intervals was either full-length precursor or fully spliced RNA (Supplementary Fig. 3a online). Partially spliced products were also virtually undetectable when subsets of the *crs1* introns were assayed (Supplementary Fig. 3b-i online). Taken together, these data support a regulatory mechanism that combines continuous transcription of the *crs1* gene with suppression of RNA processing in vegetative cells and coupled activation of polyadenylation and splicing during meiosis.

crs1 transcripts are actively turned over in growing cells

As mature mRNAs are generally more stable than unprocessed precursors22,23, it was conceivable that the increased accumulation of *crs1* RNA during meiosis was due solely to relief of the block to splicing and polyadenylation. However, the dramatic difference between the transcription and accumulation profiles of *crs1* RNA in mitotic cells (Fig. 1) suggested that an active turnover mechanism might be at work. Based on the increased levels of meiotic transcripts in vegetative cells carrying a deletion of the non-essential *cid14* gene, encoding the fission yeast orthologue of the budding yeast Trf4/5 non-canonical RNA polymerase24, we tested this strain for effects on processing and accumulation of *crs1* RNA. Notably, *crs1* transcripts remained largely unspliced and unpolyadenylated in the *cid14*Δ strain, as in wild-type cells (Fig. 3a). As Cid14/Trf4 functions in the context of the TRAMP (*T*rf4, *A*ir2 and *M*tr4 *p*olyadenylation) complex to add short poly(A) tails to nuclear substrates destined for destruction25-27, these results are consistent with our finding that *crs1* RNA is not polyadenylated in actively growing *S. pombe* cells (Fig. 2a).

The exosome, an assemblage of 3′-5′ exonucleases, has also been implicated in nuclear quality control mechanisms that affect multiple classes of RNA25. To investigate a potential role for the exosome in determining the fate of *crs1* RNA, we assayed splicing and polyadenylation in fission yeast cells harboring a deletion of the *rrp6* gene. Although *crs1* transcript accumulation was higher in this strain than in the wild type or *cid14*Δ mutant (Fig. 3a), the absence of Rrp6 also alleviated the block to both splicing and polyadenylation that normally occurs in vegetative cells (Fig. 3a). Further evidence that the nuclear exosome plays either a direct or indirect role in processing as well as turnover decisions for *crs1* is provided by the increased splicing and RNA accumulation observed in the cold-sensitive *dis3-54* mutant28 (Supplementary Fig. 4 online), encoding the catalytically active subunit29. Regulation of *crs1* thus contrasts with heterochromatic silencing, where the nuclear exosome and Cid14 function together30.

Mmi1 regulates *crs1* RNA processing as well as turnover

In seeking to identify the mechanism by which *crs1* RNA is targeted to the nuclear exosome, we noted that *crs1* was among the dozen transcripts reported to yield stronger microarray signals at the non-permissive temperature in the *mmi1* mutant, the only known *trans*-acting factor required for selective elimination of meiotic transcripts from vegetatively growing fission yeast cells31. To test whether Mmi1-mediated turnover and regulated processing of *crs1* RNA might be manifestations of the same underlying control mechanism, we assayed both available temperature-sensitive mutants for relief of the block to splicing and polyadenylation in vegetative cells. Consistent with our hypothesis, *crs1* RNA was fully processed at the non-permissive temperature in *mmi1-ts6* (Fig. 3b, left panel) and *mmi1-ts3* (Supplementary Fig. 5 online). The bypass of negative regulation was not due to elevated temperature alone, as the RNA was neither spliced nor polyadenylated in an isogenic wild-type strain subjected to the same growth regimen (Fig. 3b, right panel). Moreover, qPCR revealed that the increased accumulation of *crs1* RNA in the *mmi1-ts6* strain largely reflected an elevation of spliced RNA levels (Fig. 3c), similar to meiotic induction (Fig. 1b). The less dramatic difference (~8.5- vs. 74-fold) may reflect residual Mmi1 activity in the conditional mutants and/or the existence of additional layers of regulation.

Mutating polyadenylation factors disrupts *crs1* regulation

Based on the presence of two differentially utilized 3′ processing signals in *crs1*, we hypothesized that one or more polyadenylation factors might also function in the regulatory mechanism. An excellent candidate was Pfs2, a WD repeat-containing protein functionally related to mammalian CstF-5032, in which a temperature-sensitive mutation (*pfs2-11*) conferred a chromosome segregation defect similar to the one observed in mitotic cells over-producing spliced *crs1* mRNA2,33. Consistent with a role for Pfs2 in *crs1* regulation, shifting *pfs2-11* (Fig. 4a, left panel), but not an isogenic wild-type strain (Fig. 4a, right panel), to the non-permissive temperature led to splicing of *crs1* RNA even in non-meiotic cells. Futhermore, real-time PCR indicated that *crs1* RNA accumulation is highly elevated in this strain (Fig. 4b), comparable to the *mmi1-ts6* strain (Fig. 3c).

The increased accumulation of *crs1* RNA in the *pfs2-11* strain was surprising in that 3′ processing mutants generally led to mRNA destabilization in budding yeast34. Nevertheless, *in vivo* assays indicated that this mutation is defective for constitutive polyadenylation33, consistent with our inability to detect a poly(A) tail on the *crs*1 RNA produced in this strain (Fig. 4c, lane 1). Instead, read-through transcripts indicative of polyadenyation/transcription termination failure35 were observed, in most cases at a level comparable to the 3′ UTR control (Fig 4c, compare lane 2 with lanes 3-7). A second conditional mutant with a chromosome segregation defect similar to *crs1* over-expression, *dhp1-1*36, also led to splicing of *crs1* RNA combined with read-through transcription (Supplementary Fig. 6 online). The *dhp1* gene encodes the fission yeast orthologue of Rat1/XRN2, a 5′ to 3′ exonuclease implicated in coupling cleavage/polyadenylation to RNA polymerase II transcription termination in both budding yeast and mammals37,38. Consistent with the similar effects of *dhp1-1* and *pfs2-11* on *crs1* RNA processing and accumulation, recent data suggest an additional, earlier function for Rat1 in enhancing recruitment of 3′ processing factors39.

The proximal polyadenylation signal plays a regulatory role

To map the element(s) responsible for inhibiting *crs1* splicing during vegetative growth, we took advantage of our previous observation that intron retention was relieved upon expressing the coding region under heterologous control2. To circumvent the deleterious effects of expressing *crs1* from the *nmt1* vector2, a thiamine-responsive expression system, we inserted the coding region into an attenuated version, *nmt81*40,41 (see Methods), with the net result that the native DNA extending ∼1kb upstream from the start codon and downstream from the stop codon was replaced with vector sequences (designated NN-NN in Fig. 5a). As a control, a plasmid-borne allele carrying the same amount of native *crs1* flanking DNA was also constructed (designated CC-CC). Cells harboring this allele have a growth rate similar to wild type and are morphologically normal2.

In addition to the parental and wild type alleles, seven chimeric genes carrying different combinations of *crs1* and *nmt81* sequences in their promoter/5′UTR and 3′UTR/terminator regions were introduced into mitotically growing fission yeast cells and assayed for splicing (Fig. 5b). The recipient carried a deletion of the endogenous *crs1* gene to ensure that all signals in the assays were from plasmid transcripts. Consistent with a role for the polyadenylation machinery in regulation (Fig. 4 and Supplementary Fig. 6 online), substituting the sequences downstream, but not upstream, from the *crs1* ORF led to removal of all four introns in vegetative cells (Fig. 5b, lanes 3 & 4). More precise mapping revealed a critical role for the region encompassing the 3′ untranslated region (UTR) including both polyadenylation signals (lanes 5-8) in blocking accumulation of spliced *crs1* RNA in vegetative cells.

Given the unusual arrangement of polyadenylation sites, we next tested whether either the proximal (non-canonical) or distal (canonical) signal (Fig. 2b) present in this region is relevant to the inhibitory mechanism. Each 57 nt segment was separately replaced with complementary sequences in the context of heterologous or homologous flanking DNA. When the proximal (non-canonical) signal was ablated in a construct in which only the coding region and the segment immediately downstream were derived from *crs1* (NN-P'N), the inhibition of *crs1* splicing normally observed in mitotic cells was almost completely relieved (Fig. 5c, lane 3). In contrast, *crs1* RNA remained largely unspliced when the distal (canonical) polyadenylation signal was mutated (lane 4), as did the RNA produced from the wild type and parental alleles (lanes 1 and 2). Parallel but less dramatic results were obtained with a series of constructs in which the polyadenylation signals were mutated in the context of native *crs1* flanking DNA (Supplementary Fig. 7 online).

Based on the indistinguishable kinetics of increased *crs1* RNA accumulation and activation of splicing during meiosis (Fig. 2a & d), we asked whether substituting or mutating either polyadenylation signal increased the steady-state level of *crs1* RNA in vegetative cells. Strikingly, the proximal (non-canonical) polyadenylation signal mutant (NN-P'N) produced considerably more RNA than either the wild type (CC-CC) or parental alleles (NN-CN; Fig. 5d, compare c3 with b1 & b8). Moreover, as during meiosis (Fig. 1b), the increase was due almost entirely to a higher level of spliced RNA. In contrast, ablating the distal (canonical) polyadenylation signal depressed the level of both spliced and unspliced RNA (Fig. 5d,

compare b8 & c4). We conclude that the proximal (non-canonical) polyadenylation signal is important not only for preventing splicing, but also contributes to restricting accumulation of mature *crs1* RNA. This conclusion is bolstered by quantitative comparisons of splicing and RNA accumulation between chimeras that differ in only a single segment (Supplementary Tables 1 and 2 online).

The proximal polyadenylation signal controls 3′ processing

Given the coupling of *crs1* RNA splicing and polyadenylation during meiosis (Fig. 2e), we predicted that the non-canonical polyadenylation signal mutation (NN-P'N) would also lead to polyadenylation of plasmid-derived transcripts. Indeed, this allele produced readily detectable levels of RNA polyadenylated at the distal site (Fig. 6a, lane 3). In contrast, polyadenylated *crs1* RNA was absent in the distal (canonical) poly(A) signal mutant (lane 4), similar to wild type (lane 1), while a very faint signal was detected in the parental allele (NN-CN) (lane 2). Parallel results were observed when splicing and polyadenylation were assayed concurrently (Fig. 6b), providing additional evidence for mechanistic coupling.

The absence of a signal in the polyadenylation assay indicated that wild-type *crs1* transcripts present in actively growing cells either lack poly(A) tails altogether or possess short tails not detected under the conditions employed. To distinguish these possibilities, we tested the mutants for read-through transcription35. Transcripts extending beyond the polyadenylation signals were observed in the proximal polyadenylation signal mutant (Fig. 6c, lane 3) but not in any of the other alleles (lanes 1, 2 and 4). Moreover, using a common 5′ primer and 3′ primers complementary to sequences at varying distances downstream, read-through transcripts extending over 500 nt beyond the distal polyadenylation site were detected from both the plasmid-borne allele and the endogenous *crs1* locus (Fig. 6c). Thus, the *crs1* transcripts present in vegetative cells not only lack poly(A) tails, but are apparently not cleaved or terminated either at the polyadenylation sites used during meiosis (Fig. 2b) or for a considerable distance downstream.

A second regulatory element resides in the terminal exon

We showed previously that, although the DNA flanking the *crs1* coding region is necessary to block splicing of the native RNA during mitotic growth, it is not sufficient, as expression of otherwise constitutively spliced heterologous transcripts under *crs1* control did not block their splicing in actively growing cells2. Thus, the non-canonical polyadenylation signal is likely to function in collaboration with one or more elements that reside within the *crs1* ORF. We initially focused our search for additional regulatory sequences on the *crs1* introns, as each contains splicing signals that deviate from consensus (Supplementary Fig. 8a online); however, deletion analysis indicated that the non-canonical splice sites are not crucial for inhibition of splicing in vegetative cells (Supplementary Fig. 8b online).

Using coupled splicing/polyadenylation assays on chimeras between the *crs1* and SPAC6F6.11c genes, the second regulatory element was shown to reside within an exon. SPAC6F6.11c encodes a constitutively processed transcript similar in overall architecture to *crs1* that was previously shown to be spliced after replacement of its flanking regions with *crs1* sequences2. Substitution of *crs1* Exons 2 through 5 and their preceding introns with

SPAC6F6.11c sequences allowed RNA processing in mitotic cells (Fig. 7, lanes 2-5), while a control construct in which only the fourth intron was substituted produced no detectable fully processed RNA (lane 6), similar to wild-type *crs1* (lane 1). Because all chimeras containing *crs1* Exon 5 failed to yield product in this assay, we analyzed the effects of smaller substitutions near the 3′ end of the ORF. These experiments localized the second negative regulatory element to the penultimate 48 nt of the *crs1* coding sequence (compare lane 7 to lanes 8-11).

The sequence of the Exon 5 element provides no obvious hints as to how it might function to regulate processing of *crs1* transcripts (Supplementary Fig. 9a online). Nevertheless, assays of splicing alone also supported such a role, as all alleles lacking the native element produced spliced *crs1* RNA, albeit in variable yields (Supplementary Fig. 9b online). The similar effect of substituting this 48 nt region of Exon 5 and mutating the first *crs1* regulatory element that we discovered, the proximal (non-canonical) polyadenylation signal, prompted us to ask whether they might function collaboratively. Consistent with this hypothesis, increasing the distance between them compromised regulation (Supplementary Fig. 9c online).

Reversing polyadenylation signals compromises regulation

The presence of tandem polyadenylation signals in the *crs1* gene provided an opportunity to test the effect of switching the order in which they are encountered during transcription by RNA polymerase II. Strikingly, the Switch mutant (NN-SwN) RNA is polyadenylated (Fig. 8a, lane 1) and fully spliced (Fig. 8b, lane 3), buttressing the case for coupling of these RNA processing events. Moreover, 3′ processing of Switch mutant transcripts was efficient as judged by the absence of read-through transcription (Fig. 8a, lane 3) indicative of polyadenylation/termination failure35. The dramatic effect of the Switch mutation strongly implies that *crs1* RNA is not committed to splicing until the polyadenylation signals have been traversed by RNA polymerase II. Curiously, however, qPCR revealed that despite being fully processed, the amount of Switch mutant RNA produced was quite low (74.6 aMol/μg RNA), comparable to wild-type *crs1* or a mutant containing the native 3′ flanking region combined with *nmt81* 5′ DNA (Fig. 5d, lanes b1 & b8; Supplementary Table 2 online). A plausible interpretation is that the Exon 5 element targets *crs1* RNA for elimination, and only transcripts that escape this fate are processed.

DISCUSSION

It is now widely appreciated that the nuclear events leading from synthesis of a primary transcript to export of a mature mRNA to the cytoplasm are carefully orchestrated through a series of dynamic interactions involving multiple machines within the gene expression factory42,43. To date, the evidence for communication between the transcription apparatus and components of the splicing, polyadenylation and turnover machineries has come principally through biochemical and genetic studies of constitutively expressed genes. By analyzing a transcript that is subject to regulation, we have provided insight into how the integration of nuclear events impacts a key biological process, namely meiotic differentiation, and in the process made several unexpected observations.

We did not expect to find that the major *crs1* 3′ processing signal used during meiosis closely resembles cleavage and polyadenylation signals found in higher eukaryotes, which was unanticipated in light of earlier reports that polyadenylation in fission yeast is mediated by highly degenerate elements similar to those found in budding yeast44,45. The apparent discrepancy may be specific to the particular genes examined, or to the emphasis on transcription termination rather than polyadenylation *per se* in the earlier studies44,45. Consistent with our finding that use of the non-canonical signal is increased upon mutating it to the mammalian consensus, it has been reported that a plant polyadenylation signal containing a consensus hexanucleotide is recognized in fission yeast46.

Even more surprising was our discovery that polyadenylation of *crs1* is mechanistically linked to splicing, as coupling between these RNA processing reactions had heretofore been observed only in metazoans, and was believed to be absent from organisms that use intron definition for the initial pairing of splice sites11. It will be interesting to learn whether splicing and polyadenylation are coordinated by a conserved mechanism, as only the 3′-most intron appears to be affected in mammals47,48 whereas all four *crs1* introns are activated for splicing concurrent with *crs1* polyadenylation during meiosis (Fig. 2d) and also display parallel responses to *cis*- and *trans*-acting mutations (Figs. 3-8).

Most unprecedented was our finding that transcription of the *crs1* gene actually decreases steadily as cells enter meiotic differentiation and is near background levels when RNA accumulation peaks (Fig. 1). This observation provided the first indication that the dramatic increase in accumulation of *crs1* transcripts in meiotic cells is not merely a passive consequence of proper maturation but instead reflects an active mechanism for destroying *crs1* RNA (and presumably other *mmi1*-sensitive transcripts31) in mitotic cells. The *cis*-acting signals recognized by Mmi1 in *mei4*, *rec8*, *ssm4* and *spo5*, designated “determinants of selective removal” (DSR’s), bear no obvious resemblance to each other31 nor to the non-canonical polyadenylation signal or Exon 5 element in *crs1* (Fig. 2b and Supplementary Fig. 9a online). However, both the *crs1* regulatory elements and the majority of known DSR’s are located near the 3′ ends of the genes31. Conceivably, a conserved motif may emerge once the other elements are mapped more precisely; alternatively, it is possible that Mmi1 binds RNA in a sequence-independent manner. Our results significantly extend those reported earlier31 in that, although Mmi1 is a member of the YTH family of RNA binding proteins related to factors implicated in alternative splicing in mammals49, it was not previously known to affect splicing or polyadenylation.

The 3′ location of the *crs1* regulatory elements has two important implications. First, it distinguishes the regulatory mechanism from two previously studied fission yeast genes (*rem1* and *mes1*), in which meiosis-specific splicing is enforced by sequences that lie upstream from the coding regions7,8. While it remains to be determined whether *rem1* and *mes1* regulation are related to the well-established but as yet poorly understood ability of promoter identity to influence alternative splicing patterns in metazoans50, the shared 5′ location is suggestive. Second, the downstream location of the *crs1* control element implies that commitment of this transcript to splicing is delayed until its synthesis is virtually complete, which is remarkable in that the first intron is located over a kilobase away from the non-canonical polyadenylation signal and the Exon 5 element (see Fig 2c). One

tantalizing possibility is that processing of *crs1* RNA is promoted by juxtaposition of distant segments of the gene during meiosis, analogous to the looping observed during transcriptional induction in *S. cerevisiae*51,52.

Fig. 9 shows a working model for the roles of both *cis*-acting signals and *trans*-acting factors in regulating the maturation and accumulation of *crs1* RNA in wild-type mitotic and meiotic cells as well as the *mmi1-ts* mutant. In actively growing cells (left panel), we propose that Mmi1 nucleates formation of a complex on nascent *crs1* RNA that includes the exosome, consistent with the similar molecular signatures (increased accumulation and processing of *crs1* RNA) that we observe in the *rrp6*Δ and *mmi1-ts* mutants, as well as a two-hybrid Mmi1-Rrp6 interaction31. In that deletion of a TRAMP complex subunit has no discernible impact on *crs1* RNA processing or accumulation, the most parsimonious explanation is that in the specialized turnover pathway that blocks production of meiotic mRNAs in mitotic *S. pombe* cells, Mmi1 plays a role analogous to TRAMP-mediated polyadenylation in other nuclear surveillance and silencing pathways27,30.

Although we have not definitively proven that the *crs1* regulatory mechanism operates co-transcriptionally, several lines of circumstantial evidence support this idea. By analogy to the known association of the exosome with RNA polymerase II in *Drosophila*53, it seems plausible to suggest this mode of delivery in *crs1*. Co-transcriptional assembly of the complex that regulates turnover and processing is also consistent with the effect of reversing the order of the polyadenylation signals, as well as the involvement of Pfs2, a polyadenylation factor functionally related to mammalian CstF-50, which is known to bind the Pol II CTD42. The involvement of *dhp1* in *crs1* regulation (Supplementary Fig 6.) provides perhaps the most compelling evidence for a co-transcriptional mechanism, as its orthologues *rat1*/XRN2 link transcription termination with polyadenylation37,38. Finally, several meiotic transcripts were spliced upon lowering the gene dosage of a fission yeast cyclophilin that modulates Pol II CTD phosphorylation54, although *crs1* was not among the RNAs examined.

The middle panel of Fig. 9 depicts the proposed molecular events in wild-type *S. pombe* cells undergoing sexual differentiation. While it remains to be determined whether Mmi1 influences the delivery, stabilization or activation of the exosome in mitotic cells, in meiotic cells it cannot perform this role due to sequestration by the Mei2 protein, a key regulator of sexual development in fission yeast1,31. The functional inactivation of Mmi1 in differentiating cells renders it unavailable to bind nascent *crs1* transcripts, thus allowing them to undergo normal 3′ maturation and splicing, presumably followed by export of the mature mRNA to the cytoplasm and translation to produce the Crs1 cyclin. In *mmi1-ts* mutant cells (right panel), we propose a similar sequence of events except that a mutation rather than sequestration prevents Mmi1 from associating with newly synthesized *crs1* RNA. The molecular events in the Switch mutant are more speculative, but a plausible interpretation of the low yield of fully processed RNA is a bifurcating pathway in which destruction of the RNA competes with processing (Supplementary Fig. 10 online).

The precise role of Pfs2 is even more enigmatic, as the *pfs2-11* mutation affects constitutive as well as regulated polyadenylation, and in the context of *crs1* uncouples this RNA

processing event from splicing. One possible explanation is that splicing in *pfs2-11* (and *dhp1-1*/*rat1*, which behaves similarly) occurs post- rather than co-transcriptionally. The involvement of Pfs2 in *crs1* regulation suggests a link to control mechanisms discovered in more complex eukaryotes, as putative orthologues of this protein (CstF-50 paralogues) have been implicated in the regulation of Arabidopsis flowering55 and display increased expression during mouse spermatogenesis56. A key difference, however, is that previous studies of regulated 3′ processing, including two (non-meiotic) examples in *S. pombe*20,57-59 described switching between sites rather than the differential activation implied by our data (Fig. 2a). Based on these precedents, we fully expected a positive control mechanism in which a meiosis-specific factor would allow use of the proximal (non-canonical) polyadenylation signal; however, all of our data point instead to a negative mechanism that blocks the use of both sites in vegetative cells.

The complex, and to our knowledge unprecedented, mechanism that up-regulates *crs1* gene expression independent of transcriptional induction raises an obvious question: why do vegetative fission yeast cells continuously synthesize *crs1* RNA, only to destroy it? We propose that this regulatory strategy, in addition to preventing the deleterious production of a meiotic protein in growing cells2, serves to “prime” the gene expression pump, ensuring a very rapid response to adverse conditions in which mating, meiosis and sporulation are the organism’s sole means of survival. Given that some elements of the *crs1* regulatory mechanism have antecedents in other organisms, it is tempting to speculate that selective RNA turnover pathways may contribute more generally to changes in gene expression in response to environmental or developmental cues.

METHODS

S. pombe manipulations

See Supplementary Table 3 (online) for complete genotypes and sources for the strains used in this study. Fission yeast media and growth conditions were as described earlier2. We induced ectopic meiosis in the *pat1-114* mutant (Figs. 1 & 2) by shifting the fission yeast strain F90 to the non-permissive temperature (34°C) as described previously2. Growth conditions for other strains are described in the figure legends.

Oligonucleotides

See Supplementary Table 4 (online) for sequences of all oligonucleotides used in this study; these are grouped according to the purpose for which they were used.

Mapping the *crs1* termini

To determine the 5′ and 3′ ends of *crs1* RNA, we performed RACE (*R*apid *A*mplification of *c*DNA *E*nds) on RNA extracted from vegetatively growing or meiotic (4 h at 34°C) F90 cells. Products visible by ethidium bromide staining were cloned and sequenced by the facility at SUNY, Stony Brook.

Construction of chimeric and mutant plasmids

Due to the large number of constructs analyzed and their complexity, the relevant information is provided in Supplementary Methods online.

RNA processing assays

Processing of *crs1* RNA was assayed by both standard and real-time (quantitative) PCR. Standard (semi-quantitative) RT-PCR splicing assays were performed as described earlier2 using crs1-SAF (oligo #23) and crs1-SAR3 (oligo #68) as primers. Real-time PCR (qPCR) splicing assays were performed and the data analyzed as described in Supplementary Methods online. RT-PCR assays of polyadenylation were performed similarly except that, depending on the experimental question, two different 5′ primers (crs1-RC3′, oligo #28, or crs1-SAF, oligo #23) were used in combination with oligo$(dT)_{24}$ (oligo #69) as the 3′ primer. The 3′ UTR primer used to detect *crs1* RNA independent of polyadenylation state was crs1-nmtTRNew (oligo #17). To assay for read-through transcription, the 3′ primers were crs1-CER (oligo #70) or nmt-SEQ B2. All RNA processing assays were repeated 2-4 times using independent transformants in the case of plasmid-based experiments.

Transcription Run-On (TRO) analysis

S. pombe TRO analysis was performed essentially as described13 with the following modifications. Cells were permeabilized in 0.6% Sarcosyl (w/v) for 25 minutes with constant mixing on ice. Following this step, transcription was carried out at 30°C for 6 minutes. Equal numbers of micrograms of ^{32}P-UTP-labeled RNA from each time point was hybridized to filters on which 1.4 pmole of each denatured PCR fragment had been immobilized. The probes, which correspond to the 3′ ends of the coding region for each gene analyzed, were made by PCR using the following oligonucleotide primers (Supplementary Table 4 online): for *crs1*, crs1-nmtTR3New (oligo #19 and crs-SPAC6F-Ex5(N) (oligo #59); for *pta*1, Pta1-PF (oligo #83) and Pta1-PR (oligo #84); and for *meu*4, Meu4-DF (oligo #85) and Meu4-DR (oligo #86).

Supplementary Material

Refer to Web version on PubMed Central for supplementary material.

ACKNOWLEDGMENTS

The authors would like to thank Masayuki Yamamoto (Univ. Tokyo), Chris Norbury (Oxford Univ.) and Rich Maraia (NIH) for strains (see Supplementary Table 3 online). We are grateful to our colleagues Kristian Baker, Jonatha Gott, Hua Lou, Tim Nilsen, Cathy Patterson, Helen Salz and Steve Sanders for helpful discussions and critical reading of the manuscript. This work was funded by NIH grants R01-GM073217, awarded jointly to J. A. W. and J. L.; R01-GM064682, awarded to D. S. M.; and R01-GM38070, awarded to J. A. W.

REFERENCES

1. Harigaya Y, Yamamoto M. Molecular mechanisms underlying the mitosis-meiosis decision. Chromosome Res. 2007; 15:523–37. [PubMed: 17674143]
2. Averbeck N, Sunder S, Sample N, Wise JA, Leatherwood J. Negative control contributes to an extensive program of meiotic splicing in fission yeast. Mol Cell. 2005; 18:491–8. [PubMed: 15893732]

3. Juneau K, Palm C, Miranda M, Davis RW. High-density yeast-tiling array reveals previously undiscovered introns and extensive regulation of meiotic splicing. Proc Natl Acad Sci U S A. 2007; 104:1522–7. [PubMed: 17244705]
4. Spingola M, Ares M Jr. A yeast intronic splicing enhancer and Nam8p are required for Mer1p-activated splicing. Mol Cell. 2000; 6:329–38. [PubMed: 10983980]
5. Kishida M, Nagai T, Nakaseko Y, Shimoda C. Meiosis-dependent mRNA splicing of the fission yeast Schizosaccharomyces pombe mes1+ gene. Curr Genet. 1994; 25:497–503. [PubMed: 8082199]
6. Malapeira J, et al. A meiosis-specific cyclin regulated by splicing is required for proper progression through meiosis. Mol Cell Biol. 2005; 25:6330–7. [PubMed: 16024772]
7. Shimoseki M, Shimoda C. The 5′ terminal region of the Schizosaccharomyces pombe mes1 mRNA is crucial for its meiosis-specific splicing. Mol Genet Genomics. 2001; 265:673–82. [PubMed: 11459187]
8. Moldon A, et al. Promoter-driven splicing regulation in fission yeast. Nature. 2008; 455:997–1000. [PubMed: 18815595]
9. Cramer P, Pesce CG, Baralle FE, Kornblihtt AR. Functional association between promoter structure and transcript alternative splicing. Proc Natl Acad Sci U S A. 1997; 94:11456–60. [PubMed: 9326631]
10. Tasic B, et al. Promoter choice determines splice site selection in protocadherin alpha and gamma pre-mRNA splicing. Mol Cell. 2002; 10:21–33. [PubMed: 12150904]
11. Niwa M, Rose SD, Berget SM. In vitro polyadenylation is stimulated by the presence of an upstream intron. Genes Dev. 1990; 4:1552–9. [PubMed: 1701407]
12. Hansen K, Birse CE, Proudfoot NJ. Nascent transcription from the nmt1 and nmt2 genes of Schizosaccharomyces pombe overlaps neighbouring genes. Embo J. 1998; 17:3066–77. [PubMed: 9606189]
13. Iino Y, Yamamoto M. Negative control for the initiation of meiosis in Schizosaccharomyces pombe. Proc Natl Acad Sci U S A. 1985; 82:2447–2451. [PubMed: 16593556]
14. Mata J, Lyne R, Burns G, Bahler J. The transcriptional program of meiosis and sporulation in fission yeast. Nat Genet. 2002; 32:143–7. [PubMed: 12161753]
15. Mata J, Wilbrey A, Bahler J. Transcriptional regulatory network for sexual differentiation in fission yeast. Genome Biol. 2007; 8:R217. [PubMed: 17927811]
16. Wilhelm BT, et al. Dynamic repertoire of a eukaryotic transcriptome surveyed at single-nucleotide resolution. Nature. 2008; 453:1239–43. [PubMed: 18488015]
17. Takagaki Y, Manley JL. Complex protein interactions within the human polyadenylation machinery identify a novel component. Mol Cell Biol. 2000; 20:1515–25. [PubMed: 10669729]
18. Watanabe T, et al. Comprehensive isolation of meiosis-specific genes identifies novel proteins and unusual non-coding transcripts in Schizosaccharomyces pombe. Nucleic Acids Res. 2001; 29:2327–37. [PubMed: 11376151]
19. Gilmartin GM. Eukaryotic mRNA 3′ processing: a common means to different ends. Genes Dev. 2005; 19:2517–21. [PubMed: 16264187]
20. Liu D, et al. Systematic variation in mRNA 3′-processing signals during mouse spermatogenesis. Nucleic Acids Res. 2007; 35:234–46. [PubMed: 17158511]
21. Wilusz J, Pettine SM, Shenk T. Functional analysis of point mutations in the AAUAAA motif of the SV40 late polyadenylation signal. Nucleic Acids Res. 1989; 17:3899–908. [PubMed: 2543957]
22. Bousquet-Antonelli C, Presutti C, Tollervey D. Identification of a regulated pathway for nuclear pre-mRNA turnover. Cell. 2000; 102:765–75. [PubMed: 11030620]
23. Wilusz CJ, Wilusz J. Bringing the role of mRNA decay in the control of gene expression into focus. Trends Genet. 2004; 20:491–7. [PubMed: 15363903]
24. Wang SW, Stevenson AL, Kearsey SE, Watt S, Bahler J. Global role for polyadenylation-assisted nuclear RNA degradation in posttranscriptional gene silencing. Mol Cell Biol. 2008; 28:656–65. [PubMed: 18025105]
25. Houseley J, LaCava J, Tollervey D. RNA-quality control by the exosome. Nat Rev Mol Cell Biol. 2006; 7:529–39. [PubMed: 16829983]

26. LaCava J, et al. RNA degradation by the exosome is promoted by a nuclear polyadenylation complex. Cell. 2005; 121:713–24. [PubMed: 15935758]
27. Win TZ, et al. Requirement of fission yeast Cid14 in polyadenylation of rRNAs. Mol Cell Biol. 2006; 26:1710–21. [PubMed: 16478992]
28. Kinoshita N, Goebl M, Yanagida M. The fission yeast dis3+ gene encodes a 110-kDa essential protein implicated in mitotic control. Mol Cell Biol. 1991; 11:5839–47. [PubMed: 1944266]
29. Dziembowski A, Lorentzen E, Conti E, Seraphin B. A single subunit, Dis3, is essentially responsible for yeast exosome core activity. Nat Struct Mol Biol. 2007; 14:15–22. [PubMed: 17173052]
30. Buhler M, Haas W, Gygi SP, Moazed D. RNAi-dependent and - independent RNA turnover mechanisms contribute to heterochromatic gene silencing. Cell. 2007; 129:707–21. [PubMed: 17512405]
31. Harigaya Y, et al. Selective elimination of messenger RNA prevents an incidence of untimely meiosis. Nature. 2006; 442:45–50. [PubMed: 16823445]
32. Ohnacker M, Barabino SM, Preker PJ, Keller W. The WD-repeat protein pfs2p bridges two essential factors within the yeast pre-mRNA 3′-end-processing complex. Embo J. 2000; 19:37–47. [PubMed: 10619842]
33. Wang SW, Asakawa K, Win TZ, Toda T, Norbury CJ. Inactivation of the pre-mRNA cleavage and polyadenylation factor Pfs2 in fission yeast causes lethal cell cycle defects. Mol Cell Biol. 2005; 25:2288–96. [PubMed: 15743824]
34. Hilleren P, McCarthy T, Rosbash M, Parker R, Jensen TH. Quality control of mRNA 3′-end processing is linked to the nuclear exosome. Nature. 2001; 413:538–42. [PubMed: 11586364]
35. Proudfoot N. New perspectives on connecting messenger RNA 3′ end formation to transcription. Curr Opin Cell Biol. 2004; 16:272–8. [PubMed: 15145351]
36. Shobuike T, Tatebayashi K, Tani T, Sugano S, Ikeda H. The dhp1(+) gene, encoding a putative nuclear 5′-->3′ exoribonuclease, is required for proper chromosome segregation in fission yeast. Nucleic Acids Res. 2001; 29:1326–33. [PubMed: 11238999]
37. West S, Gromak N, Proudfoot NJ. Human 5′ --> 3′ exonuclease Xrn2 promotes transcription termination at co-transcriptional cleavage sites. Nature. 2004; 432:522–5. [PubMed: 15565158]
38. Kim M, et al. The yeast Rat1 exonuclease promotes transcription termination by RNA polymerase II. Nature. 2004; 432:517–22. [PubMed: 15565157]
39. Luo W, Johnson AW, Bentley DL. The role of Rat1 in coupling mRNA 3′- end processing to transcription termination: implications for a unified allosterictorpedo model. Genes Dev. 2006; 20:954–65. [PubMed: 16598041]
40. Basi G, Schmid E, Maundrell K. TATA box mutations in the Schizosaccharomyces pombe nmt1 promoter affect transcription efficiency but not the transcription start point or thiamine repressibility. Gene. 1993; 123:131–6. [PubMed: 8422997]
41. Maundrell K. nmt1 of fission yeast. A highly transcribed gene completely repressed by thiamine. J Biol Chem. 1990; 265:10857–64. [PubMed: 2358444]
42. Fong N, Bentley DL. Capping, splicing, and 3′ processing are independently stimulated by RNA polymerase II: different functions for different segments of the CTD. Genes Dev. 2001; 15:1783–95. [PubMed: 11459828]
43. Maniatis T, Reed R. An extensive network of coupling among gene expression machines. Nature. 2002; 416:499–506. [PubMed: 11932736]
44. Aranda A, Proudfoot NJ. Definition of transcriptional pause elements in fission yeast. Mol Cell Biol. 1999; 19:1251–61. [PubMed: 9891059]
45. Birse CE, Lee BA, Hansen K, Proudfoot NJ. Transcriptional termination signals for RNA polymerase II in fission yeast. Embo J. 1997; 16:3633–43. [PubMed: 9218804]
46. Chakraborty S, Sarmah B, Chakraborty N, Datta A. Premature termination of RNA polymerase II mediated transcription of a seed protein gene in Schizosaccharomyces pombe. Nucleic Acids Res. 2002; 30:2940–9. [PubMed: 12087180]
47. Cooke C, Hans H, Alwine JC. Utilization of splicing elements and polyadenylation signal elements in the coupling of polyadenylation and last-intron removal. Mol Cell Biol. 1999; 19:4971–9. [PubMed: 10373547]

48. Niwa M, Berget SM. Mutation of the AAUAAA polyadenylation signal depresses in vitro splicing of proximal but not distal introns. Genes Dev. 1991; 5:2086–95. [PubMed: 1657710]
49. Stoilov P, Rafalska I, Stamm S. YTH: a new domain in nuclear proteins. Trends Biochem Sci. 2002; 27:495–7. [PubMed: 12368078]
50. Kornblihtt AR. Promoter usage and alternative splicing. Curr Opin Cell Biol. 2005; 17:262–8. [PubMed: 15901495]
51. Ansari A, Hampsey M. A role for the CPF 3′-end processing machinery in RNAP II-dependent gene looping. Genes Dev. 2005; 19:2969–78. [PubMed: 16319194]
52. O'Sullivan JM, et al. Gene loops juxtapose promoters and terminators in yeast. Nat Genet. 2004; 36:1014–8. [PubMed: 15314641]
53. Andrulis ED, et al. The RNA processing exosome is linked to elongating RNA polymerase II in Drosophila. Nature. 2002; 420:837–41. [PubMed: 12490954]
54. Gullerova M, Barta A, Lorkovic ZJ. Rct1, a nuclear RNA recognition motifcontaining cyclophilin, regulates phosphorylation of the RNA polymerase II C-terminal domain. Mol Cell Biol. 2007; 27:3601–11. [PubMed: 17339332]
55. Quesada V, Macknight R, Dean C, Simpson GG. Autoregulation of FCA pre-mRNA processing controls Arabidopsis flowering time. Embo J. 2003; 22:3142–52. [PubMed: 12805228]
56. Henderson IR, Liu F, Drea S, Simpson GG, Dean C. An allelic series reveals essential roles for FY in plant development in addition to flowering-time control. Development. 2005; 132:3597–607. [PubMed: 16033802]
57. Beaudoing E, Gautheret D. Identification of alternate polyadenylation sites and analysis of their tissue distribution using EST data. Genome Res. 2001; 11:1520–6. [PubMed: 11544195]
58. Jang YK, et al. Differential expression of the rhp51+ gene, a recA and RAD51 homolog from the fission yeast Schizosaccharomyces pombe. Gene. 1996; 169:125–30. [PubMed: 8635736]
59. Munoz MJ, Daga RR, Garzon A, Thode G, Jimenez J. Poly(A) site choice during mRNA 3′-end formation in the Schizosaccharomyces pombe wos2 gene. Mol Genet Genomics. 2002; 267:792–6. [PubMed: 12207226]
60. Moreno S, Klar A, Nurse P. Molecular genetic analysis of fission yeast Schizosaccharomyces pombe. Methods Enzymol. 1991; 194:795–823. [PubMed: 2005825]

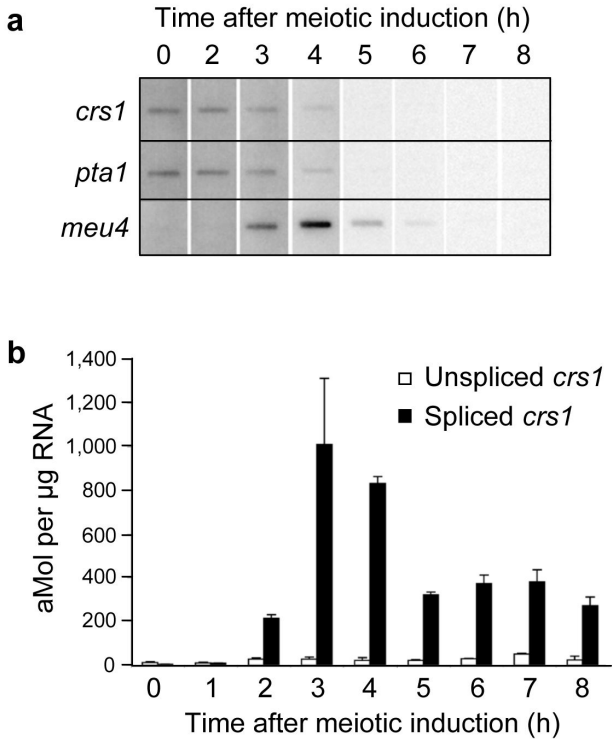

Figure 1.

Transcription of the *crs1* gene does not determine accumulation of the RNA. **a**, Transcriptional run-on (TRO) analysis of *crs1* and intronless control genes over a meiotic time course using the F90 strain containing the *pat1-114* mutation (see Supplementary Table 3 online, for the complete genotype), which undergoes ectopic meiosis at high temperature (34°C)2,12. Cells were harvested at the times indicated after induction of meiosis and the rate of RNA synthesis measured as described previously13, with the modifications noted in Supplementary Information. Newly synthesized ^{32}P-UTP-labelled RNA was detected by hybridization to probes immobilized on nitrocellulose filters followed by PhosphorImager analysis. The decreased background in the 5-8 hr TRO assays reflects the lower overall incorporation during late meiosis (D. S. M. & J. A. W., in preparation), as equal amounts of RNA (by A_{260}) were applied to each filter. **b**, Quantitative real-time PCR (qPCR) analysis of *crs1* RNA splicing over a meiotic time course. Total RNA was extracted from the F90 strain carrying a deletion of the *crs1* gene2 (see Supplementary Table 3 online for the complete genotype), and the levels of unspliced and spliced *crs1* RNA at the times indicated after the temperature shift assayed as described in Supplementary Methods (online). The absolute amount of each species in aMol per µg RNA was determined by comparison to signals generated using known amounts of T7 transcripts. All assays were performed in triplicate and error bars indicating standard deviation are shown.

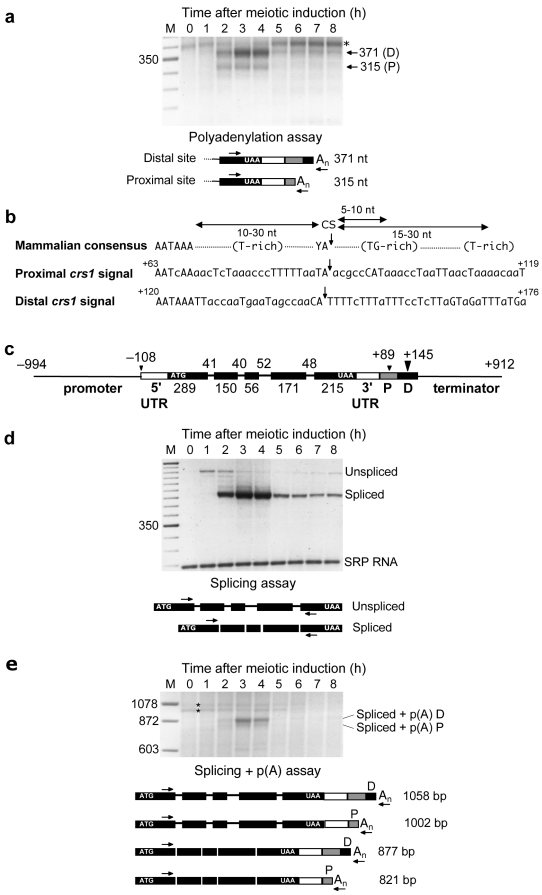

Figure 2.

Polyadenylation of *crs1* is activated concurrently with splicing during meiosis. **a**, Analysis of *crs1* RNA polyadenylation over a meiotic time course. The presence of a poly(A) tail was assessed by RT-PCR using a 5′ primer within the terminal exon and oligo(dT) as the 3′ primer as shown in the schematic; the proximal (P) and distal (D) polyadenylation signals are indicated as gray and black boxes, respectively. Assays were performed on the same RNA samples analyzed in Fig. 1b and the products visualized negatively after ethidium bromide staining. The product marked with an asterisk gave no sequence with *crs1*-specific primers and is in fact derived from an intergenic region represented in the SPAC6G9 cosmid; the absence of this non-specific band during mid-meiosis most likely reflects preferential binding of the PCR primers to *crs1* RNA. **b**, Comparison of the *crs1* polyadenylation signals to the mammalian consensus. The distances between conserved elements within the mammalian consensus are indicated at the top19,20. Within the *crs1* polyadenylation signals, nucleotides that match the mammalian consensus are shown in uppercase and non-consensus/variable nucleotides are shown in lowercase. The *crs1* sequences shown are numbered relative to the stop codon. Arrows mark the sites of *crs1* RNA cleavage/polyadenylation determined by sequencing of both cloned cDNAs and RT-PCR products. **c**, Architecture of the *crs1* locus. Promoter/termination regions are shown as lines, untranslated regions (UTRs) as open boxes, and coding exons as filled boxes. The proximal and distal polyadenylation signals are indicated as in Panel a. Arrowheads mark

RNA termini determined by RACE, numbered relative to the start and stop codons as in Panel b. **d**, Analysis of *crs1* RNA splicing over a meiotic time course. Splicing was assayed by RT-PCR on the same RNA preparations analyzed for polyadenylation in Panel a, using primers complementary to the terminal exons. SRP RNA served as an internal loading control. **e**, Concurrent assays of *crs1* RNA splicing and polyadenylation over a meiotic time course. The coincidence of the two RNA processing reactions on individual *crs1* transcripts was assessed as indicated on the diagram beneath the gel using the same 5′ primer as in Panel d and oligo(dT) as the 3′ primer. Assays employed the same RNA preparations analyzed in Panels a and d. The bands marked with asterisks migrate close to the predicted sizes of unspliced polyadenylated *crs1* RNA but gave no sequence with *crs1*-specific primers.

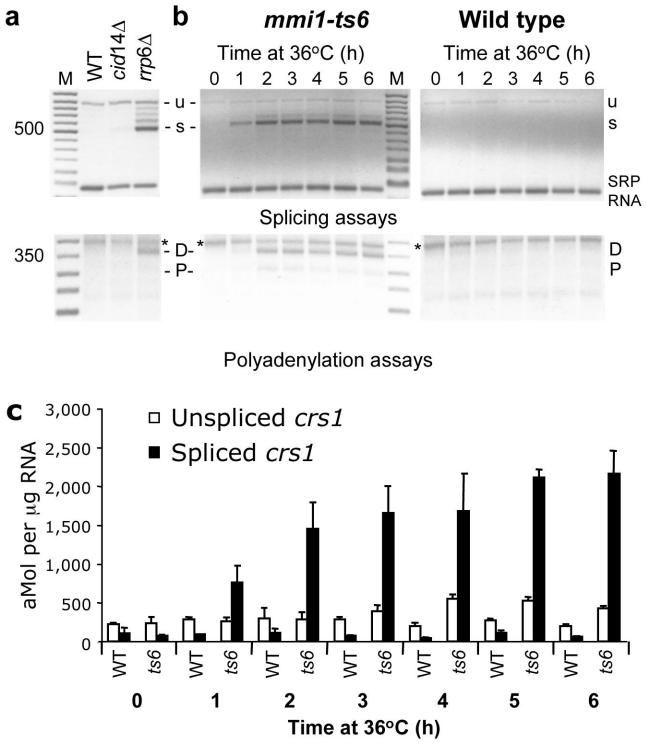

Figure 3.

The mechanism that blocks *crs1* processing in vegetative cells requires the nuclear exosome in conjunction with a factor implicated in turnover of meiotic transcripts in proliferating cells. **a**, (Top panel) Splicing of *crs1* pre-mRNA was assayed by RT-PCR as in Fig. 2d. The relevant genotype of each strain assayed is indicated above the corresponding gel lane; complete genotypes are provided in Supplementary Table 3 (online). All strains were grown at 30°C in EMM2 medium with required supplements60. (Bottom panel) Polyadenylation of *crs1* pre-mRNA was assayed by RT-PCR as in Fig. 2a, using the same RNA preparations as in Panel a. **b**,The *mmi1-ts6* mutation leads to processing of *crs1* RNA in proliferating cells. Mutant cells (see Supplementary Table 3 online, for the complete genotype) were grown to early log phase at the permissive temperature (25°C) and then shifted to the non-permissive temperature (36°C) for the indicated times. (Left panel) RT-PCR assays of splicing (top) and polyadenylation (bottom) were performed as in Fig. 2a & d. (Right panel) Splicing and polyadenylation assays on an isogenic wild-type strain subjected to the same growth regimen as the mutant strain. In the polyadenylation assays shown in both Panels a and b, an asterisk designates a product unrelated to *crs1* (see Fig. 2a legend). **c**, qPCR analysis of spliced and unspliced *crs1* in the same RNA preparations analyzed in Panel b.

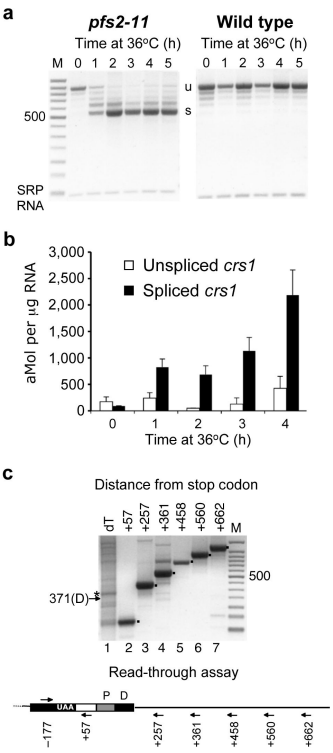

Figure 4.

The *pfs2-11* mutation leads to splicing and increased accumulation of *crs1* RNA in proliferating cells. **a**, (Left panel) RT-PCR analysis of *crs1* RNA splicing in the *pfs2-11* polyadenylation factor mutant (see Supplementary Table 3 online for the complete genotype). (Right panel) Splicing assays on an isogenic wild-type strain. Both strains were grown to early log phase at the permissive temperature (26°C) and then shifted to the non-permissive temperature (36°C) for the indicated times. **b**, qPCR analysis of spliced and unspliced *crs1* in the same RNA samples analyzed in Panels a & b. **c**, Transcripts from 3 hr *pfs2-11* (36°C) time-point that extend beyond the polyadenylation sites in the *crs1* gene were detected using a 5′ primer complementary to Exon 5 in combination with 3′ primers complementary to sequences at the indicated positions downstream from the stop codon. The product marked with an asterisk in lane 1 is described in the legend to Fig. 2a, while none of the other bands yielded sequence data with *crs1*-specific primers. In lanes 2-7, the product migrating at the predicted size for the primer pair employed in each lane is indicated by a dot.

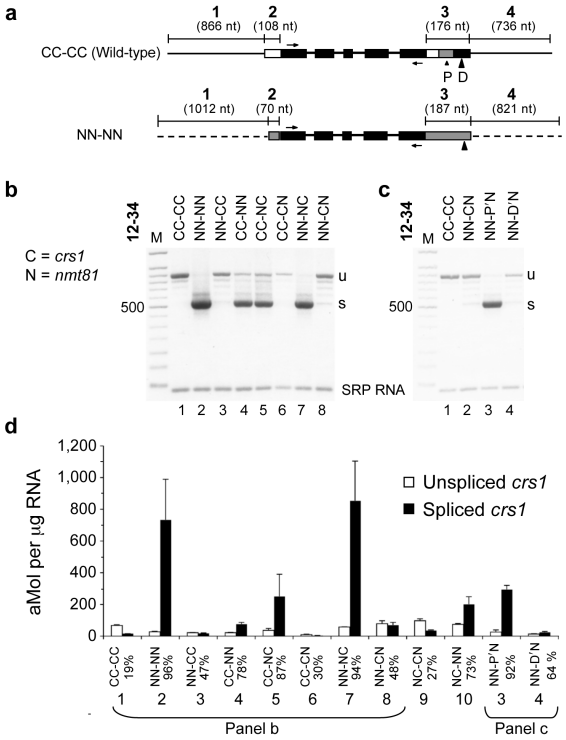

Figure 5.

The proximal (non-canonical) polyadenylation signal regulates splicing and accumulation of *crs1* RNA. **a**, Schematic diagrams indicating the regions interchanged in *nmt81-crs1* chimerae, which are demarcated by brackets and designated by numbers. **b**, RT-PCR splicing assays on *nmt81-crs1* chimerae. The letters above each lane on the gel indicate the source of the segments flanking the ORF, which correspond to the numbers on the schematic, with a dash representing the coding region. Heterologous flanking segments were derived from a thiamine-responsive expression plasmid in which the inserted ORF is surrounded by the *nmt81* transcriptional and translational control regions40,41. Analyses were carried out in the *crs1* deletion strain JLP9702 to ensure that all products were derived from the plasmid-borne alleles. **c**, Splicing assays on *crs1* polyadenylation signal mutants. Lane 1: wild-type control. Lane 2: NN-CN construct (parent for the remaining alleles). Lanes 3 and 4: either the proximal (non-canonical) or distal (canonical) 57 nt polyadenylation signal (Fig. 2b) was replaced with complementary sequences. **d**, qPCR analysis of spliced and unspliced *crs1* in the same RNA samples analyzed in Panels a-c, plus two additional chimerae (9 & 10). The percentage of spliced *crs1* RNA is indicated next to each allele designation.

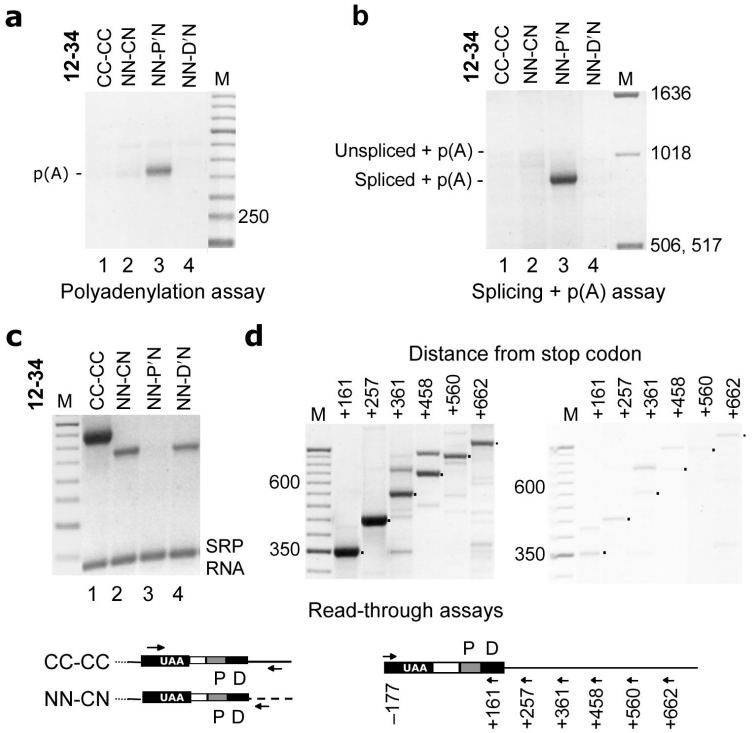

Figure 6.

The proximal (non-canonical) polyadenylation signal also regulates 3′ processing of *crs1* RNA. **a**, Assays for the presence of a poly(A) tail in *crs1* polyadenylation signal mutants. Polyadenylation was assayed as in Fig. 2a using the same RNA samples assayed for splicing in Fig. 5c. Sequence analysis indicated that the band visible in lane 3 arose via use of the distal (canonical) polyadenylation signal. The absence of the non-specific band observed in Fig. 2a may reflect production of higher levels of *crs1* RNA from multi-copy plasmids vs. the single chromosomal copy. **b**, Concurrent assays of splicing and polyadenylation in *crs1* poladenylation signal mutants. The primers employed were the same as in Fig. 2e. **c**, Assays of read-through transcription for the same mutants assayed in Panels a and b and a wild-type control. The products are of slightly different sizes (compare lane 1 with lanes 2 & 4) because, as indicated in the schematic, the 3′ primer complementary to *crs1* sequences in the wild-type allele was slightly farther downstream from the 5′ primer than was the 3′ primer complementary to *nmt81* sequences for the mutants. **d**, Assays to detect extended read-through transcripts for wild-type *crs1*. (Left panel) Plasmid-borne allele (CC-CC); (Right panel) Chromosomal allele. The 5′ primer was the same one used to assay polyadenylation while the 3′ primers were complementary to sequences within and downstream from the distal polyadenylation site. The distance from the stop codon to the end of the downstream primer is indicated above each lane of the gels and beneath the schematic diagram.

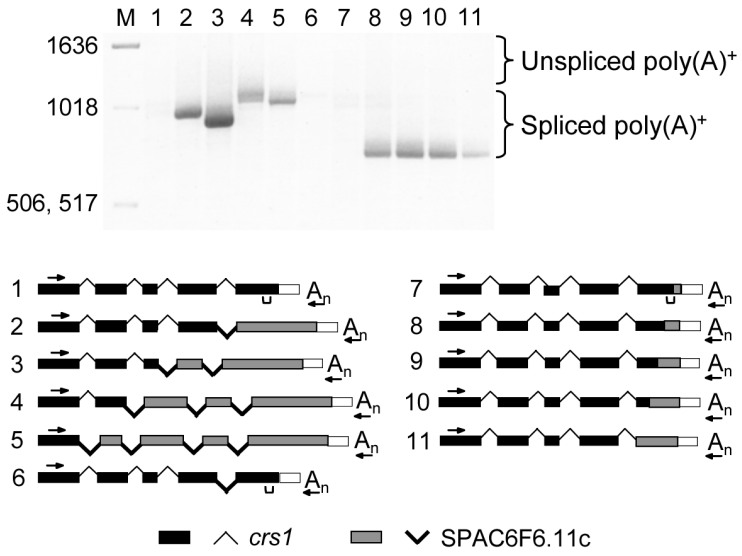

Figure 7.

An element within the fifth exon coordinately inhibits *crs1* splicing and polyadenylation. Chimerae carrying the exon/intron combinations indicated at the bottom were analyzed using a coupled splicing/polyadenylation assay as in Figs. 2e & 6b. Introns derived from *crs1* point upwards and those derived from SPAC6F6.11c point downwards and are shown in bold. A bracket beneath constructs 1, 6 & 7 indicates the location of the inhibitory sequence in Exon 5.

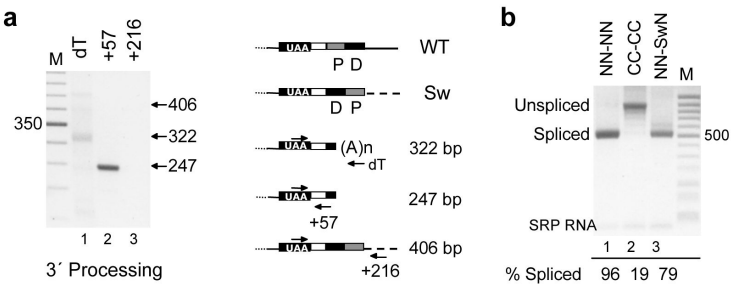

Figure 8.

Effect of reversing the order of the polyadenylation signals on *crs1* RNA processing. The proximal (non-canonical) polyadenylation signal (P) was transplanted downstream from the distal (canonical) signal (D) as described in Supplementary Information (Switch mutant). Note that this manipulation increases the distance of the non-canonical polyadenylation signal from the Exon 5 element by 57 nt. **a**, Analysis of 3′ processing in the Switch (NN-SwN) mutant. Lane 1: the presence of a poly(A) tail was assayed as in Fig. 2a. Lane 2: *crs1* RNA was detected independent of splicing or polyadenylation using a 3′ primer complementary to the 3′ UTR. Lane 3: read-through transcription was assayed by RT-PCR with the same 5′ primer used to assay polyadenylation and a 3′ primer complementary to the *nmt* sequence 68 nt downstream from the distal polyadenylation signal (see diagram). **b**, Analysis of splicing in the Switch mutant (NN-SwN) and controls are as denoted in Fig 5. Percent splicing for each allele determined from qPCR data is shown beneath the gel.

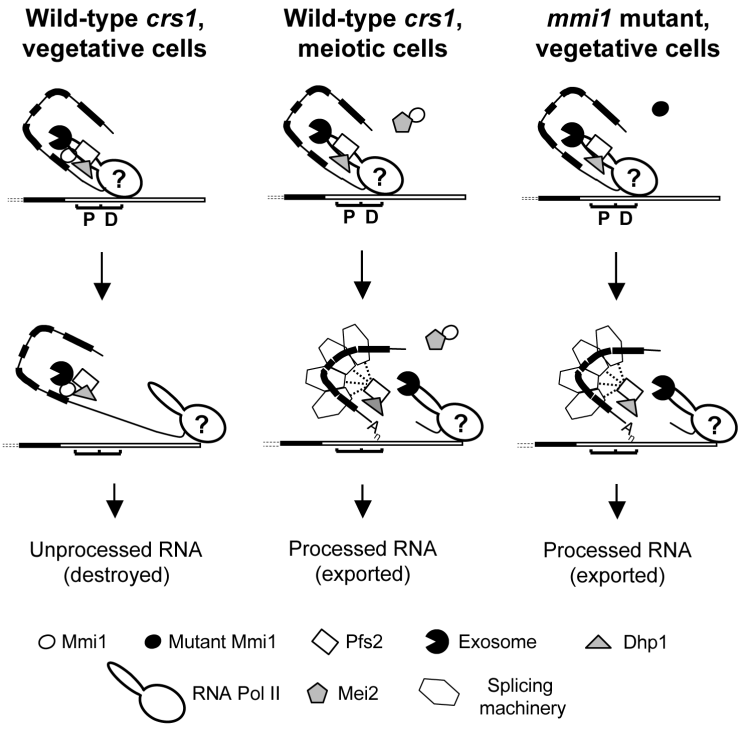

Figure 9.

Model to explain the different processing fates of the *crs1* RNA during vegetative growth and meiotic differentiation of wild-type cells and in the *mmi1-ts* mutants. The symbols representing the various factors implicated in the *crs1* regulatory mechanism are indicated in the key beneath the diagrams. The question mark over the RNA polymerase II body indicates that it has not been directly implicated in the *crs1* regulatory mechanism. As Pfs2 orthologues do not interact with RNA32 whereas orthologues of Dhp1 do39, these factors are arranged accordingly in the diagram; alternatively or in addition, it is possible that other polyadenylation factors are involved in the *crs1* regulatory mechanism. During meiosis and in the *mmi1-ts* mutants (middle and right panels), where the nascent RNA is not destroyed, the exosome is depicted as remaining associated with the elongating Pol II even though this has not been directly demonstrated.